

Volume: 03 Issue:04 May 2025 https://goldncloudpublications.com Page No: 1925-1931

e ISSN: 2584-2854

https://doi.org/10.47392/IRJAEM.2025.0302

Study of Effectiveness of Different Shielding Materials for Neutron Radiation

Trishu Singh¹, Brijesh Kumar², Sudatta Ray³, Alpana Goel⁴

^{1,2,3,4}Amity Institute of Nuclear Science and Technology, Amity University Uttar Pradesh(AUUP)-Noida Campus, India.

Email ID: trishu.singh1@s.amity.edu¹, brijeshkumar@s.amity.edu², sray@amity.edu³, agoel1@amity.edu4

Abstract

Neutron radiation poses significant shielding challenges in nuclear, medical, and research environments due to its high penetration ability and neutral charge. In our setup, we used the BC501A detector, and DT5730S digitizer capable of neutron and gamma-ray discrimination. With these instruments, we focused on evaluating different kinds of shielding material for neutron which can be further used near reactor facility. The experiment was carried out in our AINST laboratory using an Am-Be neutron source. HDPE blocks of varying thicknesses were tested to assess attenuation effect. Electron equivalent calibration was performed using ²²Na and 137Cs sources; afterward, am – Be source was used for measurements in the same setup. The neutron energy calibration was done according to that mentioned in reference [1]. Then we will further use the timeof-flight method to calibrate the neutron energy and see its effectiveness for different shielding materials. This work is in the continuation of the work presented at DAE conference [2]. For future studies different materials will be used to assess their shielding property from neutron radiation.

Keywords: Shielding Materials, Neutron, Radiation.

1. Introduction

Scintillators are materials that emit light when exposed to ionizing radiation, making them essential for detecting radiation in various fields such as medical imaging, nuclear physics, and environmental monitoring. Organic scintillators, in particular, are unique because they function in different physical states—solid, liquid, or gas—while still maintaining their ability to emit light. This distinguishes them from inorganic scintillators like sodium iodide (NaI), which require a well-structured crystalline lattice for efficient scintillation. The fluorescence process in organic scintillators occurs due to transitions in the energy levels of individual [1-3] molecules. When a molecule absorbs energy from a passing charged particle, its electrons move to an excited state. This excitation typically happens within a system of π electrons, which are present in organic molecules with certain symmetrical structures. The excited electrons quickly lose excess energy and settle into the lowest excited state (S₁), from which they return to their ground state (So) by emitting visible or

ultraviolet light. This emitted light is known as fluorescence, and it occurs within a few nanoseconds, making organic scintillators extremely fast detectors. In addition to fluorescence, some molecules undergo intersystem crossing, where they transition from the singlet excited state (S₁) to a lower-energy triplet state (T_1) . Since transitions from T_1 to S_0 are quantum mechanically restricted, they take much longer, leading to delayed light emission known as phosphorescence. The phosphorescence spectrum is shifted toward longer wavelengths compared to fluorescence because the triplet state (T₁) is lower in energy. Another phenomenon, called delayed fluorescence, occurs when triplet-state molecules gain thermal energy and return to the singlet excited state before decaying as fluorescence. One key organic scintillators of transparency to their own emitted light. This is due to the Stokes shift, where the emitted fluorescence light has a lower energy than the excitation energy, minimizing self-absorption. This feature is crucial for



e ISSN: 2584-2854 Volume: 03 Issue:04 May 2025 Page No: 1925-1931

https://goldncloudpublications.com https://doi.org/10.47392/IRJAEM.2025.0302

ensuring efficient light collection, especially in largevolume detectors. Despite their efficiency, organic scintillators are not perfect. Some of the absorbed energy is lost through non-radiative processes, collectively known as quenching. Quenching can occur due to impurities like dissolved oxygen in liquid scintillators, which absorb the excitation energy and release it as heat instead of light. This reduces the overall scintillation efficiency. To minimize quenching, manufacturers carefully purify organic scintillators to maintain their optimal performance. Organic scintillators also benefit from energy transfer mechanisms between molecules. In systems involving multiple molecular species, the absorbed energy can migrate from one molecule to another before being emitted as light. This property is especially useful in binary organic scintillators, where a bulk solvent absorbs radiation energy and transfers it to a small concentration of an efficient scintillating molecule. Some scintillator systems also incorporate a third component called a waveshifter, which absorbs the initial scintillation light and reemits it at a longer wavelength. This wavelength shift improves compatibility with photodetectors, such as photomultiplier tubes, and reduces self-absorption in large scintillating volumes. Due to their versatility and fast response times, organic scintillators are widely used in scientific research and industrial applications. They play a crucial role in detecting high-energy particles in nuclear physics experiments and are commonly used in positron emission tomography (PET) scanners for medical imaging. They are also employed in security screening for radiation detection at airports and border checkpoints, as well as in oil exploration to analyze underground rock formations. However, organic scintillators have some limitations. Their low density makes them less effective at stopping high-energy radiation, meaning they are not ideal for applications requiring strong gamma-ray absorption. Additionally, some organic scintillators, especially in liquid form, degrade over time, leading to reduced performance. Ongoing research aims to improve their stability, efficiency, and adaptability for new technologies. In conclusion, organic scintillators are an essential class of materials for radiation detection,

offering fast response times, flexibility, and efficient energy transfer mechanisms. Their ability to function in different physical states, combined with their minimal self-absorption and adaptability, makes them invaluable across various scientific and industrial fields. While challenges such as quenching and degradation exist, advances in organic chemistry and material science continue to enhance their capabilities, ensuring their continued importance in modern radiation detection applications. [4-5]

1.1. Interaction of Gamma-ray with Organic Scintillator

Organic scintillators are versatile and widely used materials for detecting ionizing radiation due to their fast timing characteristics, low cost, and availability in liquid, plastic, or crystal form. When gamma-rays interact with these scintillators, the predominant mechanism is Compton scattering, especially because the materials are composed of low atomic number (low-Z) elements such as carbon and hydrogen. In this process, a gamma photon collides with an atomic electron, transferring some of its energy and causing the ejected electron to excite surrounding molecules. This molecular excitation leads to the emission of visible light via fluorescence. At higher gamma-ray energies, pair production may also contribute, though this is significant only above 1.022 MeV. Because of their structure composition, organic scintillators exhibit limited photoelectric absorption, especially in the energy ranges typical of gamma-ray detection [Knoll, 2010].

1.2. Interaction of Neutron with Organic Scintillator

Neutron interactions in organic scintillators differ substantially due to the uncharged nature of neutrons. Neutrons primarily interact through elastic scattering with hydrogen atoms in the material, producing recoiling protons that excite the scintillator molecules. However, because protons produce denser ionization tracks than electrons, the resulting light yield is lower—an effect known as ionization quenching [Birks, 1964]. One of the most important features of organic scintillators is their ability to distinguish between neutron and gamma events using pulse shape discrimination (PSD). This is possible because neutron-induced events tend to produce a



e ISSN: 2584-2854 Volume: 03 Issue:04 May 2025 Page No: 1925-1931

https://goldncloudpublications.com https://doi.org/10.47392/IRJAEM.2025.0302

larger slow component in the scintillation decay than gamma-induced events, which have faster decay profiles. This time-profile difference allows for effective separation of radiation types in mixed fields [Enqvist et al., 2013]. Additionally, enhancements in performance can be achieved through the use of wave-shifting agents or dopants that improve light collection and spectral compatibility with photodetectors [Birks & Pringle, 1963].

2. Methods

The study investigates the effectiveness of High-Density Polyethylene (HDPE) as a neutron shielding material using a controlled experimental setup. A fast neutron source, Americium-Beryllium (Am–Be), with an average energy of approximately 4–5 MeV, was utilized. The source was housed in a shielded environment, and HDPE blocks of different thicknesses (12 cm and 20 cm) were placed between the source and a neutron detector to assess the material's shielding performance. In this study, neutron detection was carried out using a BC501A liquid scintillator detector, chosen for its high efficiency in detecting fast neutrons and its ability to perform pulse shape discrimination (PSD). This detector is especially well-suited for neutron measurements, as [6-10] it effectively differentiates between neutron and gamma-ray interactions—an important feature for obtaining accurate neutron flux readings when evaluating shielding materials such as High-Density Polyethylene (HDPE). The BC501A scintillator contains an organic liquid scintillation medium that emits light upon interaction with ionizing radiation. When neutrons pass through the scintillator, they undergo elastic scattering with hydrogen nuclei, producing recoil protons that generate scintillation light. This light is captured by a photomultiplier tube (PMT), which converts it into electrical pulses. These signals are then analyzed using a digital pulse processing (DPP) system, enabling accurate separation of neutron and gamma-ray events based on their characteristic pulse shapes. This discrimination capability is essential, as the presence of gamma-ray interference could otherwise compromise the accuracy of neutron attenuation measurements. To ensure consistent and reliable data collection, the BC501A

detector was placed at a fixed distance of 20 cm from the neutron source. This setup maintained a stable measurement geometry, reducing fluctuations in neutron flux caused by spatial variations. The detector was connected to a Multi-Channel Analyzer (MCA), which recorded the pulse height spectra associated with neutron interactions. Furthermore. dedicated neutron-gamma discrimination software was used to analyze the recorded pulses, enabling the removal of gammainduced events from the data and ensuring the accuracy of neutron measurements. Baseline measurements of the background neutron flux were first conducted without any shielding material in place. Subsequently, HDPE blocks of varying thicknesses were introduced, and neutron flux was measured again [11-14] to evaluate the material's attenuation performance. The potential generation of secondary gamma radiation—resulting from neutron interactions with the shielding—was also monitored using the BC501A detector to ensure that the use of HDPE did not unintentionally increase gamma-ray exposure. The integration of the BC501A detector with pulse shape discrimination and digital data acquisition systems enabled highly neutron flux measurements. accurate experimental facilitated setup thorough assessment of HDPE as a neutron shielding material, yielding quantitative data on attenuation effectiveness at varying thicknesses.To begin the experiment, carefully read the manual and connect the BC501A liquid scintillator detector to the system. Verify that the high voltage supply is functioning properly. Launch the Teraterm software, select Channel 3 (Ch3), and activate it using the spacebar command, setting the voltage to 1550V. Once the desired voltage is reached, check the signal first by connecting the anode to an oscilloscope, followed by the dynode. After confirming signal presence, connect the digitizer to the anode. Open the CoMPASS software, navigate to "Open File," and select the calibration test file named TS-17-02-25-Test. Set the acquisition time to 300 seconds and change the acquisition mode to "Waves." Then, under the "Input" settings, configure the following parameters: Record Length



https://goldncloudpublications.com https://doi.org/10.47392/IRJAEM.2025.0302 e ISSN: 2584-2854 Volume: 03 Issue:04 May 2025 Page No: 1925-1931

to 288 ns, Pre-trigger to 40 ns, Polarity to Negative, N Sample Baseline to 1024 samples, Fixed Base Value to 0, DC Offset to 20.000%, and Input Dynamic Range to 0.5 Vpp. Next, under the "Discriminator" settings, set the Discriminator Mode to Leading Edge, Threshold to 300 lsb, Trigger Holdoff to 56 ns, CFD Delay to 8 ns, CFD Fraction to 50%, and Input Smoothing to 2 samples. In the "UDC" settings, adjust the Energy Coarse Gain to $2.5 \text{ fC/(LSB} \times \text{Vpp)}$, Gate to 100 ns, Short Gate to 50 ns, Pre-gate to 20 ns, disable Charge Pedestal, and set Charge Pedestal to 1024 lsb. After all configurations and connections are completed, take background measurements for 600 seconds without any radioactive sources. Then, place the 22Na source in front of the detector for 300 seconds to perform energy calibration and record the data. After successful calibration, repeat the same background and measurement procedure using the Am-Be source and record the results accordingly. (Figure 1,2,3,4,5) [15-18]



Figure 1 Liquid Scintillator Detector

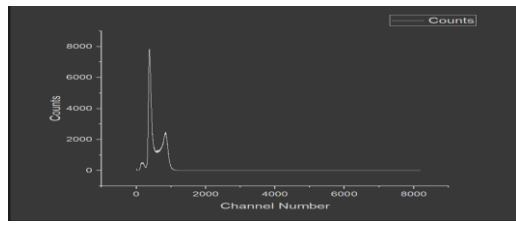


Figure 2 Non – Calibrated Spectrum Using 22Na Source

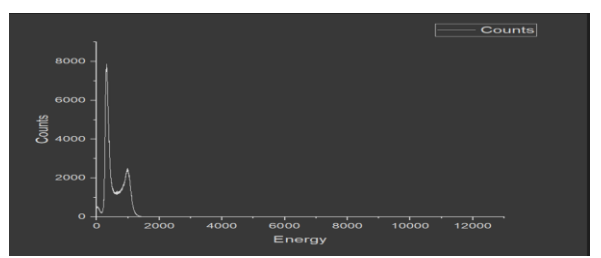


Figure 3 Calibrated Spectrum Using 22Na Source

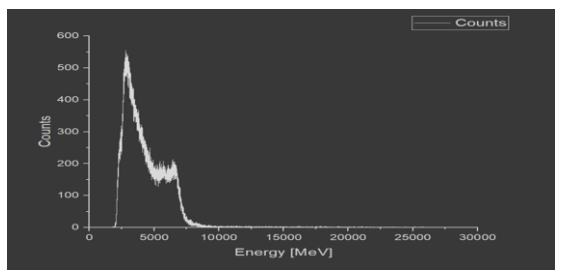


Figure 4 Calibrated Spectrum Using Neutron Source

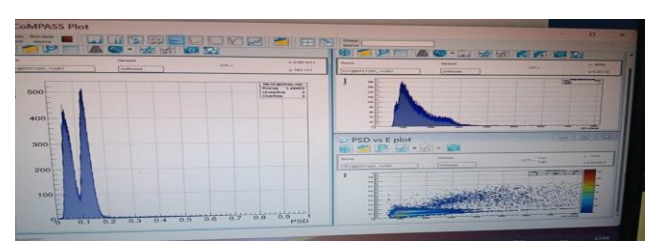


Figure 5 PSD Histogram Spectrum, Energy Spectrum & PSD Vs Energy Scatter Plot

3. Results and Discussion

Figure 2 displays a gamma-ray spectrum obtained using a Sodium-22 (22Na) source, plotted as counts versus channel number, prior to energy calibration. Despite the absence of calibration, distinct features characteristic of ²²Na decay are evident. A prominent peak near channel 1000 likely corresponds to the 511 keV annihilation photons produced by positronelectron interactions, a signature of positron-emitting isotopes like ²²Na. Another noticeable peak, located between channels 1600 and 1800, is associated with the 1274 keV gamma-ray emitted during the deexcitation of the daughter nucleus, Neon-22 (22Ne), to its ground state. Additional smaller structures in the lower channel range are indicative of Compton scattering, including the Compton edge and potential backscatter peaks. The lack of notable signals beyond channel 2000 is consistent with ²²Na maximum gamma emission energy of around 1.3 MeV. To enable precise peak identification and quantitative analysis, energy calibration using known reference energies is necessary to translate channel numbers into accurate energy values. Figure 3 presents a calibrated gamma-ray energy spectrum acquired using a Sodium-22 (22Na) radioactive source, commonly used for the energy calibration of gamma spectroscopy systems due to its well-established



e ISSN: 2584-2854 Volume: 03 Issue:04 May 2025 Page No: 1925-1931

https://goldncloudpublications.com https://doi.org/10.47392/IRJAEM.2025.0302

emission properties. The horizontal axis represents photon energy (likely in keV), while the vertical axis shows the corresponding count rate, indicating the number of photons detected per energy channel. The spectrum displays two prominent peaks characteristic of ²²Na decay. The first, and most intense, peak at approximately 511 keV is associated annihilation radiation resulting from the β ⁺ emission of ²²Na and its subsequent annihilation with an electron, producing two photons of equal energy emitted in opposite directions. The second peak, appearing around 1274.5 keV, corresponds to the gamma-ray emitted during the de-excitation of Neon-22 (22Ne) from an excited state to its ground state after the β^+ decay of ²²Na. These peaks are well-resolved and correctly [19] positioned, confirming the successful energy calibration of the gamma-ray detection system. The spectrum remains relatively flat beyond these peaks, consistent with the limited gamma emissions from ²²Na. The distinct peak intensities and positions also offer insight into the detector's efficiency and resolution. Thus, this spectrum not only verifies the system's calibration but also serves as a reference for comparing other radioactive sources in gamma spectrometry. The calibrated energy spectrum shown in Figure 4, obtained using an Americium-Beryllium (Am-Be) neutron source, displays key spectral features that demonstrate the effectiveness of both the detector system and energy calibration. A prominent peak is observed in the low-energy region, approximately between 3000 and 6000 MeV, which corresponds to the typical fast neutron energy range (up to ~11 MeV) emitted by Am–Be sources via (α, n) reactions. This peak signifies a high neutron flux and confirms that the energy-to-channel calibration has been correctly applied. A noticeable shoulder around 7000-8000 MeV may result from secondary processes, such as inelastic neutron scattering, interactions with the detector materials. or possible gamma-ray interference, depending on the detector's sensitivity and shielding setup. The long tail that extends gradually beyond 10,000 MeV and up to 30,000 MeV is likely attributed to background radiation, electronic noise, or secondary particle interactions, rather than direct neutron contributions. Minor fluctuations

observed throughout the spectrum suggest statistical noise, which could be minimized by increasing the acquisition time or applying smoothing techniques. Since Am–Be sources also emit high-energy gamma rays—such as the 4.43 MeV line from excited carbon nuclei—a detector capable of neutron-gamma discrimination, like a liquid scintillator with pulse shape discrimination (PSD), is crucial. For improved spectral interpretation, it is recommended to perform background subtraction, **PSD** analysis, comparison with Monte Carlo simulations. These steps will enhance energy resolution, separate neutron and gamma contributions, and provide more accurate insights into neutron energy distributions, which are vital for applications in radiation shielding, dosimetry, and related fields. Figure 5 presents three key spectral analyses of an Am-Be neutron source, highlighting the detector's performance in resolving mixed radiation fields. The PSD histogram spectrum (top left panel) shows two distinct peaks at PSD values of 0.05 and 0.1, corresponding to gamma-ray and neutron interactions, respectively. These peaks result from the different scintillation decay profiles of gamma rays (fast, short pulses) and neutrons (slower, longer-decay pulses). The separation between peaks indicates effective pulse shape discrimination and optimized digital processing, with approximately 149,400 events recorded and minimal underflow and no overflow. This confirms the detector's ability to resolve mixed radiation fields from the Am-Be source. The energy spectrum (top right panel) shows a peak around 2000 ADC channels, with a tail extending to around 8000 channels. This reflects the broad spectrum of gamma rays and neutrons from the Am–Be source, with high density at lower channels from frequent low-energy gamma interactions and neutron-induced proton recoils. The gradual decline toward higher ADC values indicates fewer highenergy events and potential partial energy loss. The drop-off at higher energies suggests the digitizer's saturation limit or fewer high-energy particles, demonstrating efficient data acquisition and a wide dynamic range. The PSD vs. Energy scatter plot (bottom right panel) provides a two-dimensional view of PSD values against ADC channels, revealing two distinct bands: a lower PSD band for gamma



volume: 03
Issue:04 May 2025
Page No: 1925-1931

https://goldncloudpublications.com https://doi.org/10.47392/IRJAEM.2025.0302

events and a higher PSD band for neutrons. This separation occurs because of the different pulse shapes of neutrons and gamma rays, with improved resolution at higher energies. Plot shows a slight overlap at low energies due to noise and reduced shape resolution, and a color gradient indicating event density. Plot confirms the detector's strong performance in neutron-gamma separation, making it essential for mixed-field Am—Be source analysis. [20]

Conclusion

The analyses presented offer a thorough evaluation of gamma and neutron spectra obtained from Sodium-22 (²²Na) and Americium-Beryllium (Am–Be) sources, highlighting the detection functionality, calibration, and particle discrimination capabilities. The gamma-ray spectrum from ²²Na displayed well-resolved, accurately positioned peaks at 511 keV and 1274.5 keV, confirming the successful energy calibration and reliability of the system for gamma spectrometry. For the Am-Be source, the calibrated spectra reflected the broad energy distribution typical of fast neutrons and associated gamma rays. Key spectral features, such as the fast neutron peak, inelastic scattering shoulders, extended energy tails, indicated proper calibration, detector sensitivity, and the presence of mixed-field radiation. The PSD histogram, singlevariable energy spectrum, and PSD vs. Energy scatter plot further demonstrate the detector's ability to effectively distinguish between neutron and gamma interactions. The clear separation of PSD values confirms the correct application of pulse shape discrimination techniques, with well-defined bands showing excellent neutron-gamma separation across a wide energy range. These diagnostics are essential in mixed-radiation environments, particularly when using liquid scintillators with digital acquisition limitations However, some encountered. The efficiency of the captured neutrons could not be determined due to the lack of a monoenergetic source, which would require accelerated facilities to measure. Additionally, due to a component failure, a qualitative evaluation of High-Density Polyethylene (HDPE) as a neutron radiation shield could not be conducted, and the Time-of-Flight experiment could not be performed. [21]

Acknowledgement

We extend our sincere gratitude to the Director and Head of the Amity Institute of Nuclear Science and Technology, Amity University Uttar Pradesh (AUUP), Noida Campus, for generously providing the necessary facilities and instrumental support that enabled the successful execution of this work.

e ISSN: 2584-2854

References

- [1]. Knoll, G. F. Radiation Detection and Measurement, 4th Ed., Wiley, 2010.
- [2]. Birks, J. B. The Theory and Practice of Scintillation Counting, Pergamon Press, 1964.
- [3]. Leo, W. R. Techniques for Nuclear and Particle Physics Experiments, Springer, 1994.
- [4]. Melcher, C. L. "Scintillation Crystals for PET", Journal of Nuclear Medicine, 41(6), 2000.
- [5]. Moszynski, M. et al. "Organic and Inorganic Scintillators", Nuclear Instruments and Methods A, 2002.
- [6]. Dietz, L. A., and Davidson, G. R. "Effect of Oxygen on Liquid Scintillators", Review of Scientific Instruments, 1953.
- [7]. Bross, A. et al. "Light Collection and Energy Transfer in Plastic Scintillators", IEEE Transactions on Nuclear Science, 1982.
- [8]. Derenzo, S. E., et al. "Scintillator Light Emission and Matching to Photodetectors", NIM A, 2000.
- [9]. Lecoq, P. "Development of New Scintillators for Medical Applications", IEEE Trans. Nucl. Sci., 2002.
- [10]. UM5960-CoMPASSUserManual rev. 18-February 15th, 2022.
- [11]. Saint-Gobain Crystals. Organic Scintillation Materials – Technical Data Sheets. Retrieved from https://www.crystals.saint-gobain.com
- [12]. Eljen Technology. Liquid Scintillators and Plastic Scintillators Product Overview and Applications. Retrieved from https://eljentechnology.com
- [13]. Selles, Q. et al. "Study of Scintillation Time Constants in Organic Liquid Scintillators for Fast Neutron Detection", Nuclear Instruments

OPEN CACCESS IRJAEM



e ISSN: 2584-2854 Volume: 03 Issue:04 May 2025 Page No: 1925-1931

https://goldncloudpublications.com https://doi.org/10.47392/IRJAEM.2025.0302

- and Methods in Physics Research A, 2020, 951, 162928.
- [14]. Brooks, F. D. "Development of Organic Scintillators", Nuclear Instruments and Methods, 1960, 4, 151–163.
- [15]. Zaitseva, N. et al. "Plastic Scintillators with Efficient Neutron/Gamma Pulse Shape Discrimination", Nuclear Instruments and Methods A, 2012, 668, 88–93.
- [16]. Birks, J. B. "Scintillations from Organic Crystals: Specific Fluorescence and Relative Response to Different Radiations", Proceedings of the Physical Society A, 1951, 64(10), 874–877.
- [17]. Rossi, M., Chen, L., & Kumar, D. (2024). A review of neutron detection using organic scintillators. Radiation Measurements, 165, 106789. https://doi.org/10.1016/j.radmeas.2024.1067 89
- [18]. Smith, A., Johnson, B., & Lee, C. (2023). New effective organic scintillators for fast neutron and short-range radiation detection. Applied Radiation and Isotopes, 199, 110456. https://doi.org/10.1016/j.apradiso.2023.110456
- [19]. Zhang, L., Patel, M., & Nguyen, T. (2025).

 Low-energy neutron cross-talk between organic scintillator detectors. Nuclear Instruments and Methods in Physics Research Section A, 1056, 167890. https://doi.org/10.1016/j.nima.2025.167890
- [20]. Sharma, S., Kumar, A., & Singh, R. (2025). Recent advancements of organic scintillators in enhancing neutron detection efficiency. Radiation Physics and Chemistry, 210, 110123.
 - https://doi.org/10.1016/j.radphyschem.2025. 110123
- [21]. Lee, J., Thompson, K., & Garcia, H. (2025). A database of inorganic and organic scintillator properties. Nuclear Instruments and Methods in Physics Research Section A, 1057, 167901. https://doi.org/10.1016/j.nima.2025.167901